US Department of Energy, National Energy Technology Laboratory

In-Operando Evaluation of Solid Oxide Fuel Cell (SOFC) Cathodes for Enhanced Oxygen Reduction Reaction (ORR) Activity and Durability

Project Period: 10/01/2015 - 06/30/2017

PI: Eric D. Wachsman, Ph.D.
Director, University of Maryland Energy Research Center
William L. Crentz Centennial Chair in Energy Research
University of Maryland
College Park, MD 20742
ewach@umd.edu
Tel.: (301) 405-8193, Fax.: (301) 314-8514

Submission Date: March 30, 2018

Award No. DE-FE0026190

Submitting Official: Stephanie M. Swann
Contract Manager
University of Maryland
Office of Research Administration
3112 Lee Building
College Park, MD 20742
smbrack@umd.edu
Tel.: (301) 405-8079, Fax.: (301) 314-9569
DUNS Number: 790934285

TABLE OF CONTENTS

Abstract

Through this project we developed a new *in-operando* ^{18}O-isotope exchange technique, and determined the oxygen reduction reaction (ORR) kinetics and mechanisms in various solid oxide fuel cell (SOFC) cathodes under real operating conditions of applied voltage. We were able to measure and determine oxygen surface exchange coefficients of labeled oxygen with $La_{0.8}Sr_{0.2}MnO_3$ (LSM), $La_{0.6}Sr_{0.4}Co_{0.2}Fe_{0.8}O_3$ (LSCF) and other cathode material samples with varying compositions. We related the cell polarization conditions to the surface exchange process and surface exchange coefficient, and suggested a model to describe this relation. Our findings imply that LSCF keeps its higher exchange rate performance over LSM under real operating conditions. Changing the A-site cation ratio in LSM can enhance its performance, especially under cathodic polarizations larger than -400mV. Cathode powder composites of LSM and LSCF with YSZ and GDC show lower exchange coefficient values under applied polarization compared to the single constituent powder samples, probably due to limited contact between the powder particles. Using our model and basic electrochemical properties of the cathode materials we are able to successfully predict the exchange kinetic properties of SOFC cathode material under real operating conditions of applied voltage / current from surface exchange coefficients obtained in the absence of an applied bias.

1. Background

Cathode performance and durability are still the critical issues in commercialization of SOFC technology. In order to optimize cathode performance and durability, data collection under real working conditions is crucial. We previously pioneered, through NETL Contract No. DEFE0009084, a multi-faceted fundamental investigation of the effect of contaminants, such as H_2O, CO_2, and chromium vapor, on cathode performance degradation mechanisms, in order to establish composition/structures and operational conditions for the enhancement of SOFC cathode durability.[1-5] We determined the microstructural and compositional changes upon exposure to those contaminants using the combination of electrochemical impedance spectroscopy (EIS) and focused ion-beam scanning electron microscopy (FIB-SEM). Furthermore, based on isotope exchange we determined the different reaction mechanisms on relevant

material systems, different oxygen transport pathways in composites, and dominant gas-solid reactions while multiple gases are present. Our findings show H_2O and CO_2 active participation in the ORR on ion-conducting materials such as LSCF, GDC, and YSZ. In the low and intermediate temperature regions (<500°C), H_2O and CO_2 exchange are the dominant reactions over oxygen exchange on these solid surfaces. In contrast, H_2O and CO_2 reactivity on LSM is limited. In addition, we observed that H_2O and CO_2 reactivity is dramatically enhanced in composite cathodes, attributed to the high defect concentrations at the interfaces between solid phases.

Our research yields fundamental understanding of the cathode degradation mechanisms, attributable to typical contaminants, such as water,[2] CO_2 ,[5] and Cr,[1] and validated approaches to mitigate them. Hence, our results provide a clear path for overcoming the hurdle that cathode performance stability has been to SOFC technology implementation. However, these earlier results were achieved in the absence of an applied bias that occurs in working SOFC's. Therefore, under this contract we developed a novel *in-operando* isotope exchange apparatus and performed experiments for SOFC cathode material powders, in real-time and under real-life operating conditions, that allow the design of cathode compositions with enhanced performance and durability. Combining these analysis techniques together with an in-depth study on cathode properties under real operation conditions (*in-operando*) provides a clearer picture of the degradation mechanism in different scales, from 3D micron scale reconstruction to nano scale kinetic reactions.

2. Approach

Throughout this project the effect of cathodic bias on the surface oxygen exchange activity of SOFC cathode materials was investigated. Powder samples of different compositions were tested under a variety of bias voltages, temperatures and pO_2's. The major goals and objectives of the project are:

- Develop an *in-operando* ^{18}O-isotope exchange apparatus for the study of SOFC cathodes oxygen surface exchange properties, under operating conditions of applied voltage / current.

- Determine surface exchange mechanisms and coefficients using *in-operando* ^{18}O-isotope exchange apparatus for LSM and LSCF powders with varying compositions, and their composites with YSZ and GDC.

3. Experimental Setup

In order to achieve the goals of this study, a new design of our oxygen isotope exchange apparatus was developed and adjustments to an *in-operando* mode were taken. The new design enables measurement of oxygen exchange reactions of SOFC cathode powders under applied voltage and current. The powder sample is placed in a tube-shaped plug flow micro-reactor (Figure 1). The feed stream, containing a mix of $^{16}O_2$, $^{18}O_2$, Ar and He, flows over the powder, exits the reactor, and is sampled by mass spectrometer, which records the changes in the *32* ($^{16}O_2$), *34* ($^{16}O^{18}O$) and *36* ($^{18}O_2$) m/z signals. In order to apply bias and achieve oxygen ionic transport, the plug flow micro reactor was made from YSZ tube. One electrical contact to the powder (working electrode) is provided by an Au-coated thermocouple tube. The second electrical terminal is through Pt coating on the outer surface of the YSZ tube.

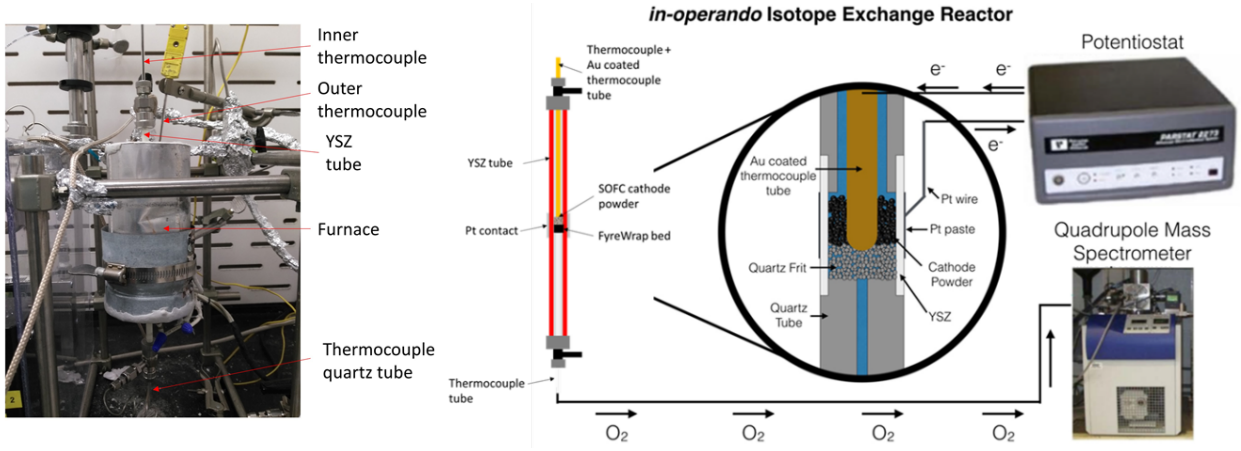

Figure 1. Photo and schematic of *in-operando* isotope exchange system consisting of YSZ tube flow reactor, connected to mass spectrometer. Electrical leads are through Au coated thermocouple tube in the center of cathode powder sample and Pt coating on outside of YSZ electrolyte tube.

4. Results and Discussion

Exchange profiles

Using the above described configuration, oxygen isothermal isotope exchange (IIE) experiments of various SOFC cathode materials under polarization were conducted. The materials included LSM and LSCF with varying site ratio and doped with additional cations. The experimental conditions varied were cathodic polarization and temperature.

Figure 2 (a) displays an example for the oxygen exchange profiles of LSCF, under zero bias and under a potential bias of -500mV at 450°C. At this temperature, LSCF is not under limitation of $^{18}O_2$ supply from the gas stream,[6-7] therefore any difference in the oxygen profiles can be attributed to the effect of

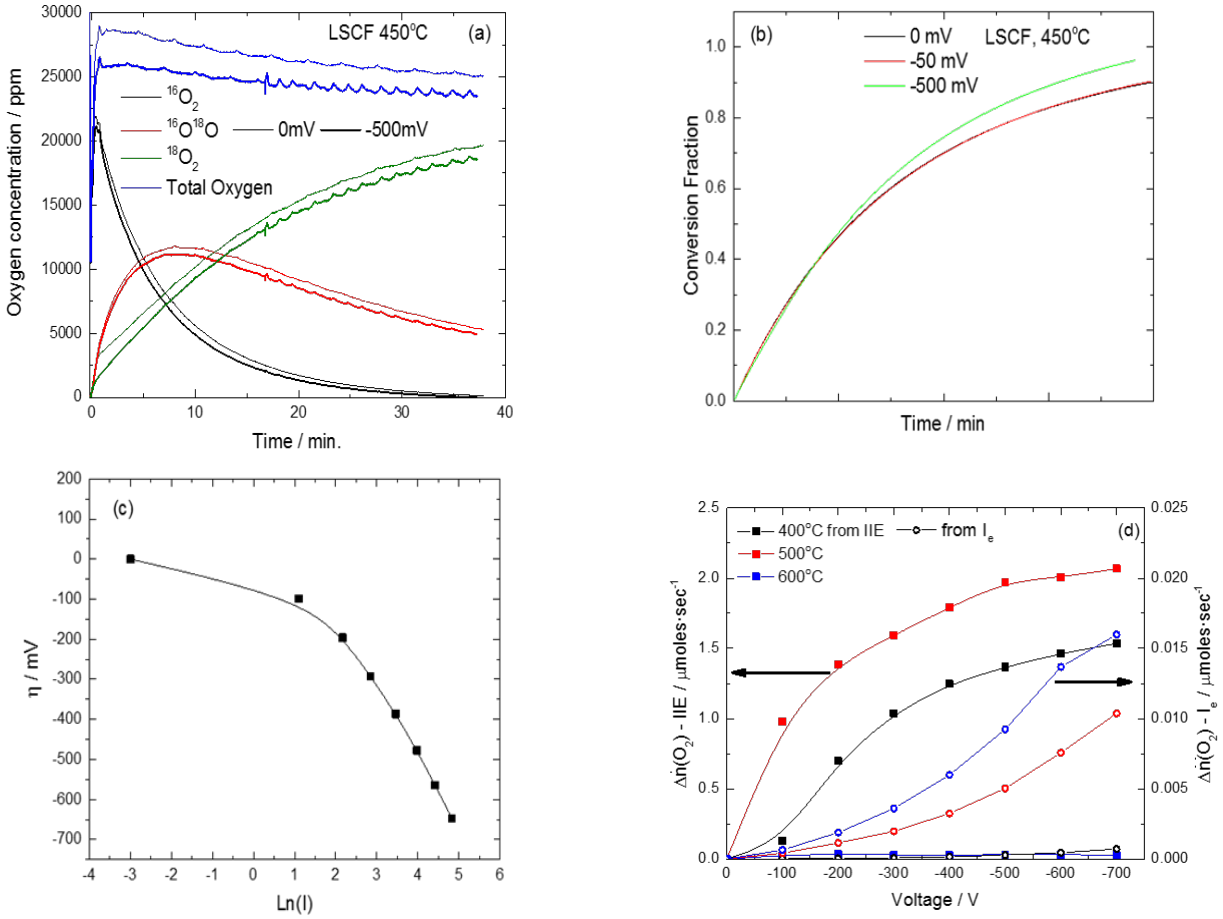

Figure 2. (a) Oxygen isotope exchange curves for LSCF with and without the application of cathodic polarization, at 450°C, (b) corresponding conversion fraction plots, (c) Tafel plot for LSCF at 450°C. (d) Oxygen flux as a function of applied cell potential as determined by mass spectrometer analysis of gas phase (IIE) and Faradaicly by cell current (I_e).

applied polarization. Figure 2 (b) shows the corresponding ^{18}O accumulation curves, obtained from the IIE curves in Figure 2 (a). As can be seen, the conversion fraction of $^{18}O_2$ increases with the increase in polarization, which indicates a higher conversion rate for the case when polarization is applied. Figure 2 (b) also includes the conversion fraction curve obtained under low polarization of -50mV. At -50mV, the polarization has only negligible effect, therefore no difference can be detected in the conversion fraction curve between 0mV and -50mV. Figure 2 (c) shows the I-V electrochemical characteristics of LSCF at 450°C, measured in this apparatus, in a Tafel plot. The curve shape follows a classic electrochemical reaction, thus it serves as a confirmation that the application of polarization results indeed in the promotion of an electrochemical reaction.

To further investigate this effect and also to separate out the effect of cell current (I_e) from observed impact of polarization on *in-operando* measured (IIE) exchange kinetics we compared the oxygen flux ($\Delta n^{\bullet}(O_2)$) obtained by the IIE measured difference between the oxygen concentration under applied cathodic polarization vs. that at OCP, with that of the Faradaic oxygen flux (I_e) due to electrochemically pumping O_2 out of the cell, as a function of cell voltage for LSCF at various temperatures (Figure 2 (d)). As can be seen from data on right, the I_e induced oxygen flux ($\Delta n^{\bullet}(O_2) - I_e$) increases with increasing applied cell voltage consistent with the Tafel data for this LSCF/YSZ/Pt cell (Figure 2 (c)). In addition, as the temperature increases the YSZ resistance decreases and thus the cell current and corresponding induced oxygen flux ($\Delta n^{\bullet}(O_2) - I_e$) increases, with negligible flux for any applied bias investigated at 400°C and a flux of ~0.015 $\mu moles \cdot sec^{-1}$ at -700 mV and 600°C.

In contrast to I_e, the IIE induced oxygen flux ($\Delta n^{\bullet}(O_2)$ - IIE) has a dramatically different voltage relationship and temperature dependence. Whereas the oxygen flux due to current ($\Delta n^{\bullet}(O_2) - I_e$) increases exponentially with voltage resulting in a Tafel expected concave up profile, the IIE induced oxygen flux ($\Delta n^{\bullet}(O_2)$ - IIE) has a concave down profile indicating a completely different polarization mechanism. Further, the temperature dependence is completely different with ($\Delta n^{\bullet}(O_2)$ - IIE) at 400° and 500° C, and dramatically higher than ($\Delta n^{\bullet}(O_2)$ - IIE) at 600°C. This demonstrates that it was not an effect of current

which had strong temperature dependence, but rather an effect of the exchange kinetics for LSCF. At 600°C oxygen IIE on LSCF surface is limited not by the kinetics of the LSCF itself, but rather limited by reactants supply from the gas stream. Moreover, the O_2 flux from IIE is two orders of magnitude higher than that from I_e clearly demonstrating that our *in-operando* approach was probing the impact of polarization on heterogeneous kinetics and not the effect of current.

In a similar manner to the method described for LSCF, we were able to determine the isotope oxygen exchange process on the surface of LSM powder. Figure 3 displays the $^{18}O_2$ accumulation profiles for LSM at 450 and 600° C. Again, we can see a great effect of polarization on the accumulation curves. Even though LSM is relatively poor oxygen ionic conductor, application of polarization causes an increase in the conversion fraction at each temperature.

Calculation and modeling of exchange rate coefficient:

In order to quantify the oxygen exchange process, and to achieve better understanding of the effect of polarization on the oxygen mechanism, we need to extract the oxygen exchange rate coefficients from the oxygen isotope exchange curves. This will provide us with a reliable tool to compare the activities of different materials under different operating conditions. So far, our analysis of the oxygen exchange curves was based on fitting of the conversion fraction curves to a reaction rate model equation.[3] However, since

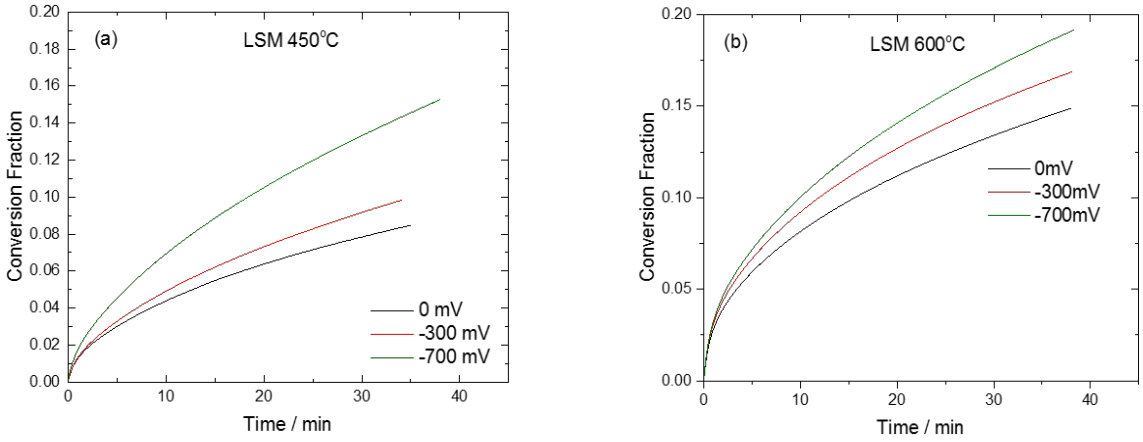

Figure 3. Conversion fraction curves for LSM at (a) 450, and (b) 600° C under various cathodic polarizations.

this project involves the addition of an electrochemical polarization to the measurement procedure, we should also introduce an electrical current or an electrical potential term to our model. Our modification is based on the un-biased model, which has been proven to reliably support and represent the oxygen exchange. To adjust this model, we introduce a component which expresses the promotion of the exchange processes as a result of the conduction of charge carriers (electrons, oxygen ions) through the cathode material and the YSZ electrolyte tube. The ions that participate in the oxygen surface exchange, and travel through the material due to the application of electrochemical potential are oxygen ions O^{2-}, including ^{18}O isotopes. They promote, or depress, the oxygen exchange through their formation or destruction on the surface. The exchange rate depends now not only on the rate in which $^{18}O_2$ molecules are absorbed on the surface, but also on the rate in which they are reduced and move into the bulk material as $^{18}O^{2-}$. Our model for the exchange is based on the following assumptions:

1. Dissociative adsorption of $^{18}O_2$ is proportional to the fraction of available sites on the surface, θ.
2. The "consumption" of $^{18}O_2$ on the surface is proportional to the fraction of occupied sites, $1-\theta$.
3. Both reactions are of first, or pseudo-first, order.

The first assumption describes the dissociative adsorption reaction, with a 2-D reaction rate constant R_{ex}. The applied polarization is effective through the second assumption, with the relevant term *I/2FN*, as being used in the analysis of the electrochemical promotion of catalysis (EPOC) processes.[9] Based on the above assumptions, the time dependent $^{18}O_2$ coverage is:

$$(t) = \frac{I/2F}{(I/2F) + R_{ex}N}\left[1 - e^{-\left(\frac{I}{2FN} + R_{ex}\right)t}\right] \qquad (1)$$

According to Equation 1, the concentration of accumulated $^{18}O_2$ exponentially increases with time under polarization, with a similar form of exponential growth as the solution for the non-biased case, as also demonstrated in Figures 2 (b) & 3. However, the accumulated $^{18}O_2$ also increases with the applied current / polarization.

The 2-D surface exchange rate coefficient, R_{ex}, is related to the more common used parameter, surface exchange coefficient (k_{ex}) through the following relation:

$$R_{ex} = 6k_{ex} / D \tag{2}$$

where D is the diameter of the cathode powder sphere particle. Therefore, we can obtain the 3-D surface exchange rate coefficient, k_{ex}, for the case of measurement under polarization, by fitting the accumulation plot to the exponential growth form in Equation 1:

$$k_{ex} = \frac{D}{6} \; b \; \frac{I}{2FN} = \frac{D}{6} \; b \; \frac{I_0 \exp(C \;)}{2FN} \tag{3}$$

where b is a fitting parameter from the accumulation curve. Figure 4 displays the dependence of the exchange coefficient k_{ex} for LSCF and LSM on the electrode overpotential η. As can be seen, the exchange rate coefficient increases with increase in the cathodic polarization. The difference in the exchange coefficient becomes more dominant under larger overpotentials, while with small overpotential values (0 to -400mV) the change is relatively small, especially at lower temperatures.

The next question to be asked is whether we can somehow generalize the dependence of the surface exchange coefficient on the applied potential, and use this to predict and learn from the performance of cathode materials under operation conditions. One way to do so is by employing the electrochemical

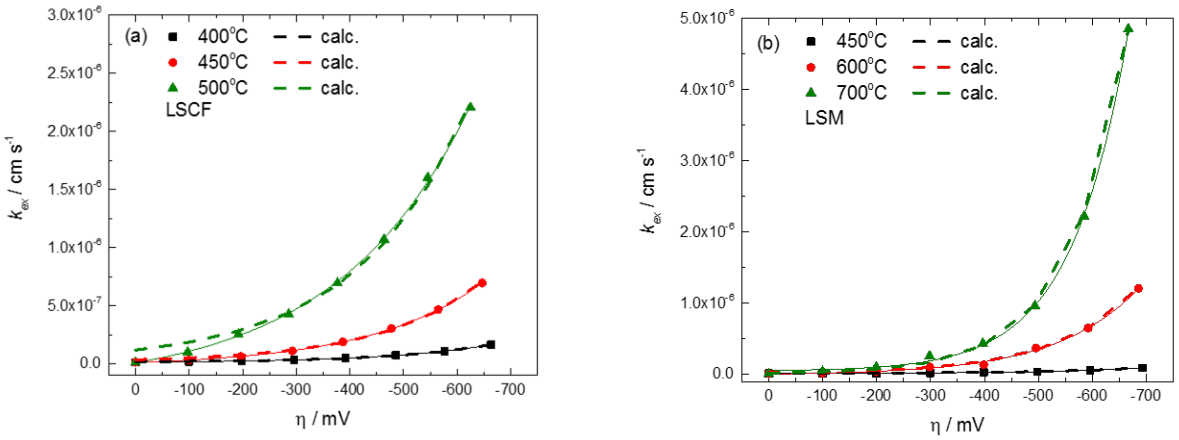

Figure 4. Exchange rate coefficient dependence on applied cathodic polarization of (a) LSCF, and (b) LSM. Solid thin line: Curve fitting according to Equation 3. Bold dash line: Calculated values obtained from k_{ex} at OCP, using electrochemical parameters from Tafel plot.

parameters I_0 and C in Equation 3. These parameters are pure electrochemical parameters, independent of the isotope exchange process, and therefore can be measured and determined separately, regardless of the $^{18}O_2$ exchange experiment. We can use the Tafel equation which relates the overpotential to the current, in order to extract these two electrochemical parameters:

$$I = I_0 \exp\left(\quad F \quad / RT \right) = I_0 \exp\left(C \quad \right) \tag{4}$$

We used the Tafel plot, generated using our electrochemical setup, and extracted the parameters I_0 and C for the cathode materials under investigation. Using these parameters from the Tafel relation we were able to plot the corresponding line, following Equation 3. These fitting lines are displayed in Figure 4 (bold dashed lines), and are in very good agreement with the experimental data. These results demonstrate that we can successfully predict the surface exchange coefficient of cathode materials under cathodic polarization, based on k_{ex} obtained at OCP. This provides the first-ever capability to use literature surface exchange coefficients obtained at OCP, together with pure, independent electrochemical properties, to calculate the surface exchange under applied cathode polarization.

Figure 5 summarizes of the calculated dependence of the oxygen surface exchange coefficient k_{ex} on cathodic polarization for LSM, LSCF, and two more LSM- and LSCF-based compositions, with variations in the ion composition at A and B sites: $La_{0.6}Sr_{0.3}Co_{0.2}Fe_{0.8}O_{3-x}$, (LSCF-A) with 30% of Sr in the A-site, compared to 40% Sr in the LSCF, and $(La_{0.65}Sr_{0.35})_{0.95}MnO_{3-x}$ (LSM-D), an LSM-based material with a change in the A-site composition compared LSM $(La_{0.8}Sr_{0.2})_{0.95}MnO_{3-x}$. In all the materials the change with respect to the magnitude of the applied polarization is minor until polarizations of around -300 to -400 mV, however at higher polarizations the increase is of few orders of magnitude. These results indicate that applied cathodic polarization improved dramatically the surface exchange properties of the investigated materials. Moreover, while under OCP conditions one material performs better than another, under real operation conditions this trend can change, for example LSCF and LSCF-A. Investigations on the effect of applied polarization on composite cathode materials, as well as on other cathode materials, are currently in progress.

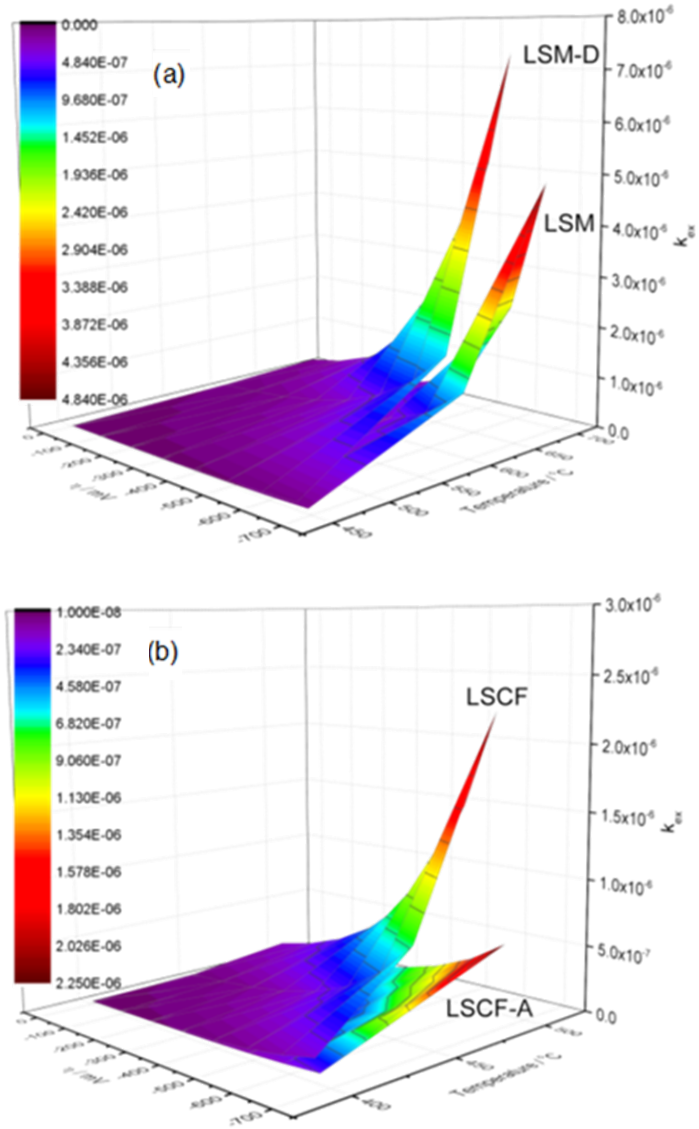

Figure 5. Calculated exchange rate coefficient dependence on applied cathodic polarization of (a) LSM and LSM-D, and (b) LSCF and LSCF-A.

As the results in Figure 4 show, the calculated lines of the surface exchange coefficient are in very good agreement with the experimental values. Therefore, the developed model, based on Tafel relation, describes correctly the processes and the resulting surface exchange coefficients. Moreover, since the electrochemical parameters can be determined separately from the oxygen isotope exchange measurements, the surface exchange coefficients can be accurately predicted under any given temperature and polarization. However, the Tafel relationship is an approximation for large overpotential as can be seen in Figure 6 (a), where the measured exchange coefficients of LSCF at 500°C and of LSM at 700°C are compared to the

predicted values in a logarithmic scale. In this case the level of agreement between the measured and predicted surface exchange coefficient values is lower at low polarizations. This is true not only for these two specific materials under investigation, but is also observed with other materials investigated with the *in-operando* system over a wide range of temperatures. Under small polarizations, known as "resistance polarization", the logarithmic relation is not applicable, therefore the prediction does not follow the measured values. Under this region, the correct equation to describe the relation is the simplified version of the Butler–Volmer equation for low overpotential:

$$I = I_0 \frac{zF}{RT}\left(E \quad E_{eq}\right) = I_0 \frac{zF}{RT} \tag{5}$$

where E_{eq} is the equilibrium potential. Figure 6 (b) presents the Ln(k_{ex}) vs. η results for LSM and LSCF, however this time the calculated line of Ln(k_{ex}) is calculated using the linear Butler-Volmer relation (Equation 5) at small polarizations, and the regular Tafel equation at higher polarizations. The distinction between the two ranges was determined based on the Tafel plot for each material and temperature set. The relevant polarization / current value was estimated as the value in which the η-Ln(I) curve deviated from linearity. As can be seen, the level of agreement between the two sets of surface exchange coefficient, measured and calculated, is significantly better, especially for the case of LSCF. This serves as another

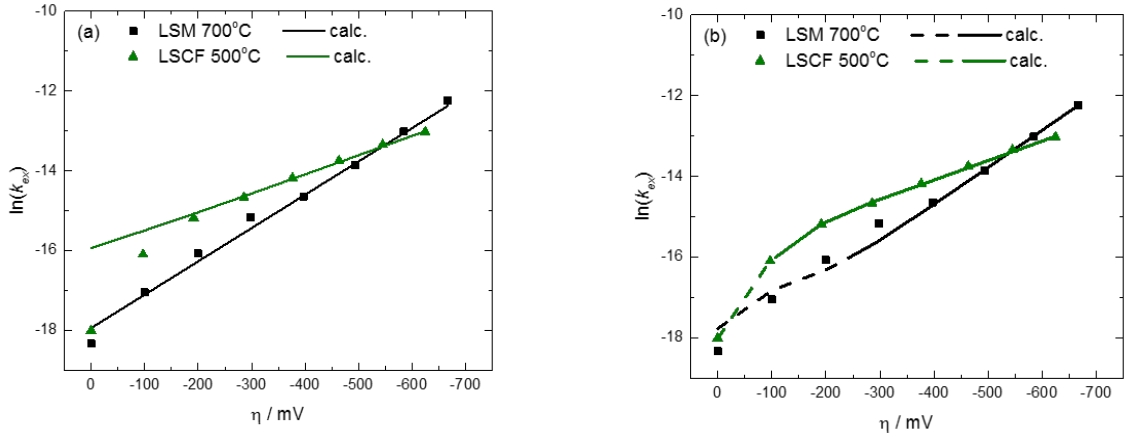

Figure 6. Oxygen exchange coefficient dependence on the cathodic polarization and temperature on a logarithmic scale for LSM 700°C and LSCF 500°C. Line: calculated values using electrochemical parameters using (c) Tafel equation over entire polarization range, and (d) linear Butler-Volmer relation for low polarizations (dash line) and Tafel equation for high polarizations (solid line).

indication that our *in-operando* experimental setup enables monitoring evolved gasses and measurement of surface exchange reactions, while inducing and controlling electrochemical conditions.

The oxygen surface exchange profiles were examined for other SOFC cathode materials of the ABO_3 perovskite structure, with variations in the identity and concentration of A- and B-site occupants - $(La_{0.8}Sr_{0.2})_{0.95}CoO_{3-\delta}$ (LSC) and $(La_{0.6}Sr_{0.4})_{0.95}FeO_{3-\delta}$ (LSF). Both LSC and LSF are mixed ionic electronic conductors (MIEC), therefore they should have similar properties as LSCF, which is a MIEC as well. Previous studies reported that values of k_{ex} for LSC are 1-2 orders of magnitude higher than k_{ex} for LSF.[10-13] However, these reported experimental results were measured using depth profiling or conductivity relaxation methods, which lack the surface sensitivity that the surface exchange technique that is reported here can provide. The surface exchange process measured with these methods is measured either under the diffusion-limited regime of the exchange process, or under the mixed diffusion-surface regime, due to the use of sample thickness. The isotope oxygen exchange technique provides the opportunity to measure the surface exchange process under pure surface-controlled regime, since the particle size is considerable smaller. Using this technique, the obtained surface exchange properties of LSC and LSF are very similar, which demonstrates that the measured *k* is indeed a different property for the different techniques, however the isotope exchange enables obtaining pure surface exchange coefficients. The nature of the B-site cation, whether it is Fe or Co, has a small effect on the exchange properties of these two MIEC materials. This can be seen in Figure 7 (a), which compares the oxygen exchange profiles of LSC and LSF at 600°C. Both materials show similar shapes of $^{16}O_2$, $^{16}O^{18}O$, and $^{18}O_2$ signals, indicating that the overall oxygen surface exchange process is similar in these two MIECs. The electrochemical characterization of LSC and LSF at various temperatures is shown in Figure 7 (b). The results clearly verify that incorporating LSC and LSF in the YSZ tube of the *in-operando* setup serves as a complete electrochemical cell and that similar to their exchange results (Figure 7 (a)) they have similar electrochemical response (Figure 7 (b)).

The effect of applied polarization on the oxygen surface exchange coefficient and validation of the suggested model were examined with the other SOFC cathode materials, LSF and LSC. Figure 8 shows the exchange coefficient of LSC and LSF, as a function of overpotential, at various temperatures. The trend in

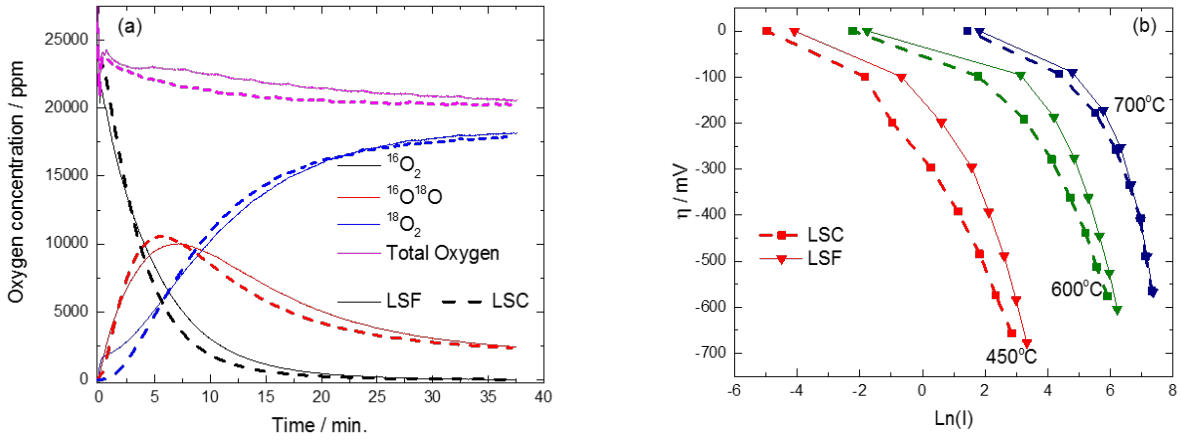

Figure 7. (a) Oxygen isotope exchange profiles at zero potential, 600°C for LSC and LSF. Both materials are MIEC, showing similar ORR kinetic properties. (b) Electrochemical characteristics of LSC and LSF in YSZ-tube/Pt cell at 450°C, 600° C, and 700°C.

exchange coefficient with temperature and polarization is similar. Figure 8 also includes predicted values for the oxygen surface exchange coefficient, based on the suggested model, incorporating the electrochemical parameters of the cathode materials based on Tafel relation. As can be seen, for LSC and LSF there is a very good correlation between the measured values and the calculated values. Figures 8 (c) and (d) display the dependence of the logarithm of the exchange coefficient on applied polarization for LSC and LSF. The distinction between low polarization values, where the Butler-Volmer equation is valid, and the high polarization range where Tafel relation is the effective one, leads to high accuracy in the prediction of the exchange coefficient for these two materials as well.

A complete picture for the dependence of surface exchange coefficient on temperature at OCP for LSCF, LSM, LSC, and LSF is presented in Figure 9 (a). As can be seen, LSC shows the highest exchange properties among the investigated materials when no polarization is applied. The predominance of LSC in terms of surface exchange coefficient was previously observed with isotope exchange experiments.[6] All materials show the expected increase in surface exchange coefficient with temperature, with positive values of activation energy.

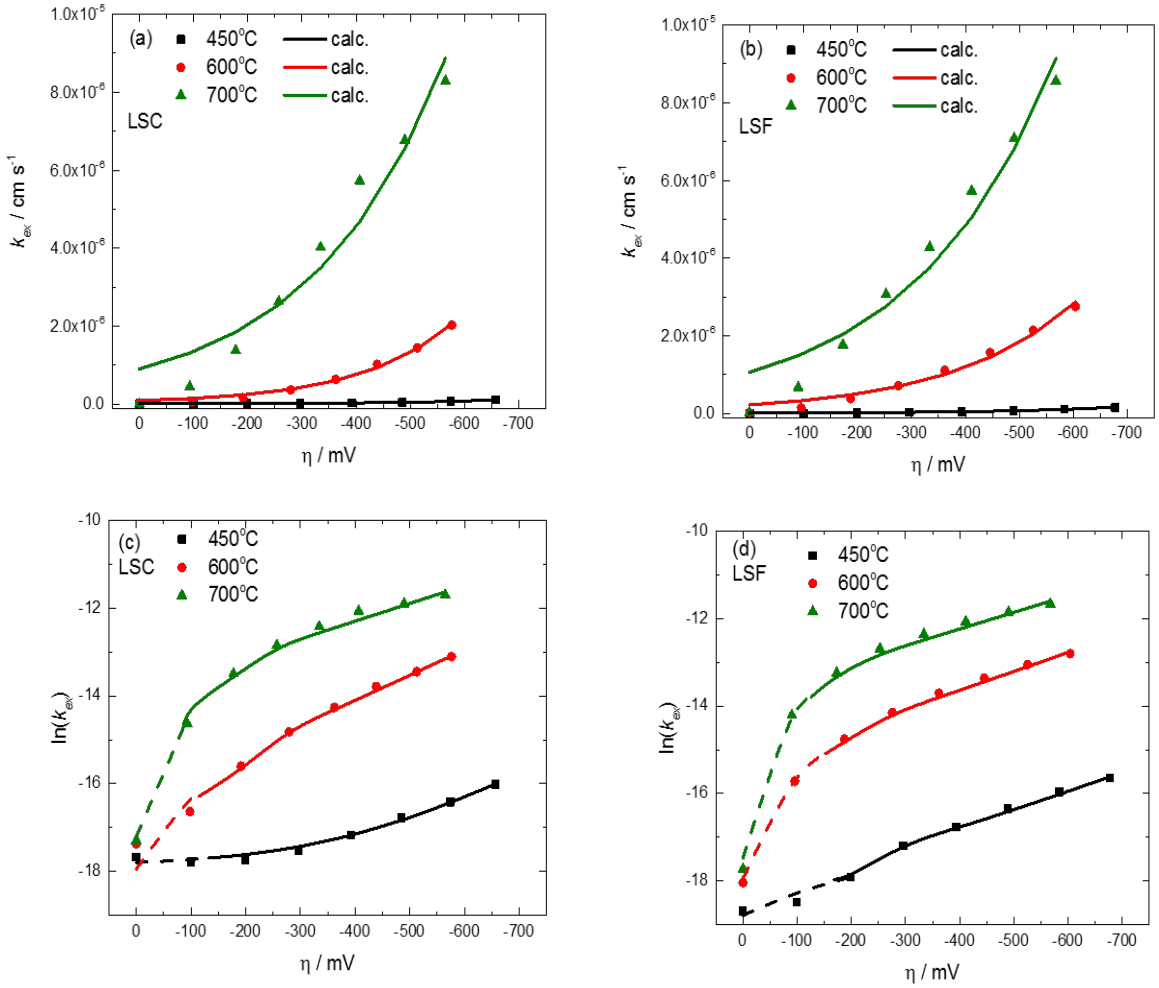

Figure 8. Dependence of oxygen exchange coefficient on the cathodic polarization and temperature for (a) LSC and (b) LSF. Solid lines calculated using electrochemical parameters from Tafel plots. (c) & (d) Oxygen exchange coefficient dependence on the cathodic polarization and temperature on a logarithmic scale for LSC and LSF, respectively, at 450, 600, and 700°C. Dash line: calculated following Butler-Volmer relation. Solid line: calculated following Tafel relation.

Figures 9 (b) and (c) compare the oxygen surface exchange of LSF, LSC, and LSM variation with overpotential at 600°C and 700°C. As can be seen, at both temperatures LSM shows the lowest surface exchange coefficient over the entire potential range. However, it is important to note that under no polarization, as displayed in Figure 9 (a), LSC shows the higher kinetic properties for oxygen surface exchange. On the other hand, when polarization is applied, LSC is inferior in its surface exchange values to LSF indicating the importance of comparing material properties under anticipated working polarization.

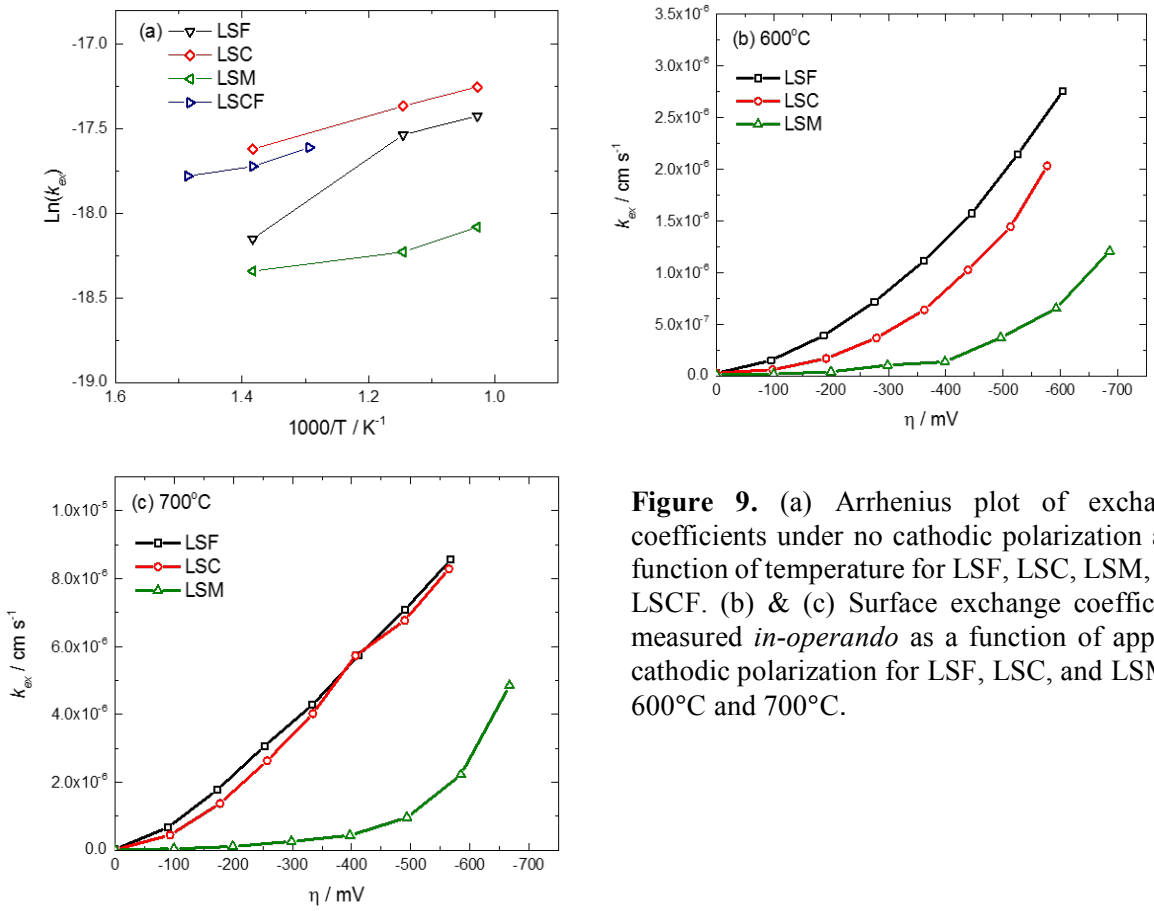

Figure 9. (a) Arrhenius plot of exchange coefficients under no cathodic polarization as a function of temperature for LSF, LSC, LSM, and LSCF. (b) & (c) Surface exchange coefficient measured *in-operando* as a function of applied cathodic polarization for LSF, LSC, and LSM at 600°C and 700°C.

We also examined and studied the combined effect of composition and applied cathodic polarization on the surface exchange properties of LSM and LSCF composites with YSZ and GDC. Figure 10 (a) displays the dependence of the exchange rate coefficient k_{ex} for LSCF-GDC composite at 400, 450, and 500°C. As can be seen, the exchange rate coefficient increases with the increase in the cathodic polarization and with the increase in exchange temperature. Figure 10 (a) also includes predicted values for the oxygen surface exchange coefficient, based on our model, incorporating the electrochemical parameters of LSCF-GDC composite. As can be seen, the agreement between the measured values and the predicted values, according to this model, is very weak, especially with increase in temperature. This correlation is notably poor when we compare it to other SOFC cathode materials that are described previously in this report. In the previous cases, where the investigated materials were homogeneous and not composites, the

correlation between the model and the experimental results was very good. This enabled us to pre-determine the oxygen surface exchange coefficient under operating conditions based on the performance at OCP, together with electrochemical characterization of the sample. The noticeable difference is probably due to the difference between the two types of materials under investigation, one of perovskite-based SOFC cathode materials, and the second of a composite of the cathode oxide with an electrolyte material (GDC or YSZ). The addition of another material, creating a two-phase material, limits the validity of our model. The model is based on reaction limited by surface exchange and not by diffusion or conduction mechanisms within the bulk material or on the boundary between the different phases. Figure 10 (b) presents the Ln(k_{ex}) vs. η results for LSCF-GDC, including the predicted values (dash lines) resulted from using the Butler-Volmer relation low polarization region and Tafel relation for higher polarization values. As can be seen in Figure 10 (b), using this method the correlation between the measured data and the predicted values is much better, mainly in the low polarization range. This serves as another indication that the Tafel relation should be reconsidered when treating surface exchange coefficient data for composites.

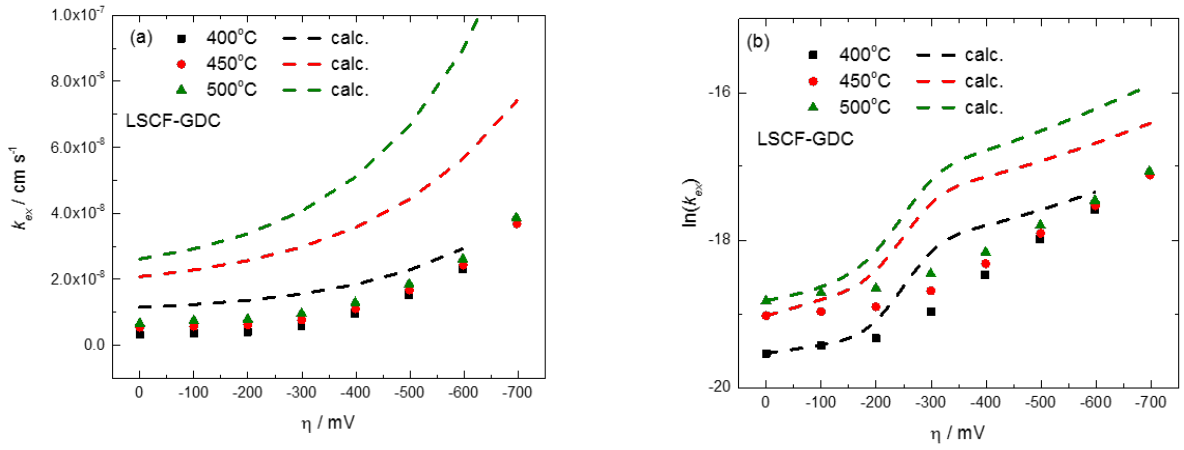

Figure 10. (a) Dependence of oxygen exchange coefficient on the cathodic polarization and temperature for LSCF-GDC composite. Solid lines calculated using electrochemical parameters from Tafel plots. (b) & (d) Oxygen exchange coefficient dependence on the cathodic polarization and temperature on a logarithmic scale for LSCF-GDC. Dash line: calculated following Butler-Volmer relation. Solid line: calculated following Tafel relation.

Figure 11 displays the surface exchange coefficient of LSM-YSZ and LSM-GDC composites, and its variation with the applied polarization. In a similar manner to the case of other composite (LSCF-GDC) described in Figure 10, the agreement between the measured values and the ones predicted through our model is very weak. However, for the case of LSM-YSZ (Figure 11 (a)), there is almost no dependency of the surface exchange coefficient on the applied cathodic polarization. These two materials, LSM and YSZ, are considered pure electronic and pure ionic conductors, respectively. For LSM, there are no available oxygen vacancies to mitigate the exchange. YSZ on the other hand lacks the needed electrons for the exchange process. Our previous studies, as descried in our previous reports, show that these two materials exchange oxygen very slowly separately. LSM alone shows lower surface exchange properties compared to the MIEC LSCF, however the application of cathodic polarization on LSM has altered its exchange abilities. In a composite powder form, when LSM is mixed together with YSZ, there is not enough intimate interface between the two components of the composite. The lack of interface hinders any conduction mechanism between the two materials and therefore within them. Presumably, the combination of this two materials with high conductivity, ionic in the YSZ and electronic in the LSM, should lead to high surface exchange properties of the composite. However, this is true only if there is enough active interface between the two constitutes. Since this is not the case for the composite powder under our investigation, the resulted performance is poorer. LSM-GDC (Figure 11 (b)) exhibits much stronger dependence on the applied polarization, when its surface exchange coefficient increases with higher cathodic polarizations. However, the matching between the measured values to the predicted values is still low. Unlike YSZ, GDC is a MIEC, therefore the combination with the pure ionic conductor LSM creates better conditions for full exchange reaction, compared to the LSM-YSZ combination, hence higher surface exchange coefficient properties. The difference in exchange mechanism between the two composites can also be seen in Figure 11 (c), which displays the exchange curves of the two materials. As can be seen, the evolution with time of each of the oxygen species, $^{16}O_2$, $^{16}O^{18}O$, and $^{18}O_2$, is different for the two different composites. The rise of $^{18}O_2$ signal for LSM-YSZ is much more rapid than that of LSM-GDC, indicates that much lesser number of exchange

events are occurring in the LSM-YSZ composite. This also indicates that the exchange process is much slower for LSM-YSZ than for LSM-GDC composite. This difference can also be seen in the $^{16}O_2$ signal, indicating that the exchange mechanism is completely difference between the two materials. In a similar manner to LSCF-GDC, the acquired surface exchange coefficient for LSM-based composites was also compared to the model based on both Tafel relation at high polarizations and Butler-Volmer relation at low polarizations. Figures 11 (d) and (e) include the variation in Ln(k_{ex}) under different cathodic polarizations, together with the predicted values of the surface exchange coefficient using the suggested model. As can be seen, the level of agreement between the two sets of surface exchange coefficient, measured and calculated, is higher compared to the calculation method described in Figures 11 (a) and (b).

To achieve a better understanding on the degradation mechanism of SOFC cathode materials under operating conditions, we performed aging tests for the cathode materials. Aging tests were performed at the highest temperature that oxygen isotope surface exchange experiment is observable and effective. For LSCF-GDC this temperature is 500°C, while above this temperature incorporation of oxygen into the lattice is too fast that the exchange process is gas-diffusion limited by the supply of $^{18}O_2$ reactant from the gas phase, and not by the actual heterogeneous exchange ability of the material. Therefore, above 500°C the both application of polarization, higher temperatures, and aging time on LSCF-based materials cannot measurably change the exchange rate. For LSM-based materials, the aging temperature was set on 700°C. Aging of cathode samples was performed in two different manners. The first method was aging the sample outside of the tube furnace, at a constant temperature of 700°C, for 230 to 240 hours. This is a higher temperature than that used to test the oxygen exchange reaction itself, however, as previous studies of us show,[(1)] high temperature should increase the rate of degradation process, if there is any. The second mode of aging was performed inside the YSZ tube at a lower temperature of 500°C for LSCF-based materials, or 700° C for LSM-based materials. This mode enables the application of cathodic polarization on the powder sample along the aging process. This allows us to examine whether the application of continuous polarization has an effect on the oxygen exchange properties of the cathode material.°

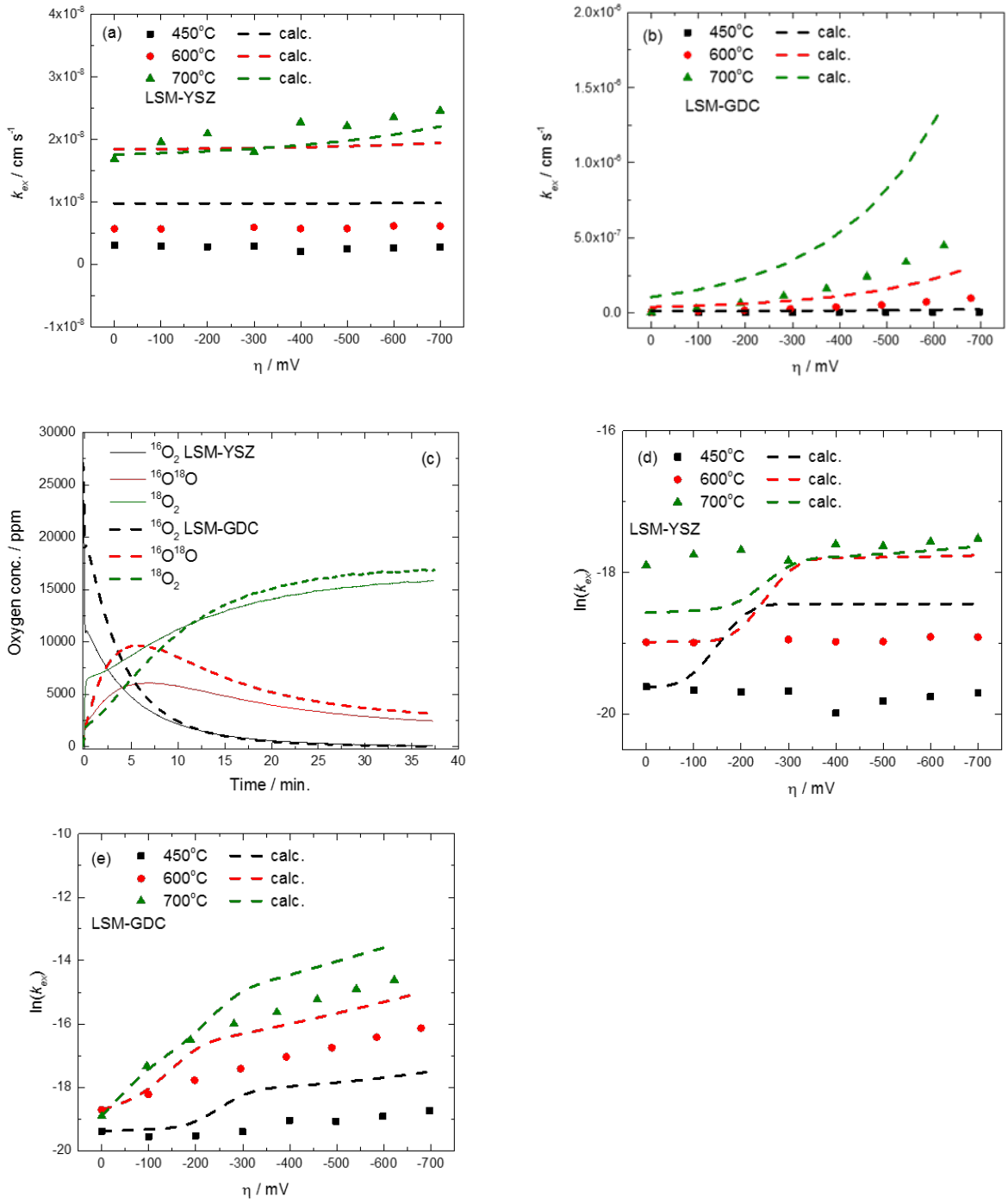

Figure 11. (a) Dependence of oxygen exchange coefficient on the cathodic polarization and temperature for (a) LSM-YSZ, and (b) LSM-GDC composites. Solid lines calculated using electrochemical parameters from Tafel plots. (c) Oxygen isotope exchange curves for LSM-YSZ and LSM-GDC at 600°C, η=0mV. Oxygen exchange coefficient dependence on the cathodic polarization and temperature on a logarithmic scale for (d) LSM-YSZ and (e) LSM-GDC. Dash line: calculated following Butler-Volmer relation. Solid line: calculated following Tafel relation.

Figure 12 (a) displays the oxygen exchange curves of LSCF-GDC performed at 500°C under cathodic polarization of -300mV. The oxygen exchange properties were tested at the beginning of aging (t=0), and after 137 hours of aging at 500°C, under polarization of -300mV. This value of polarization was chosen as an intermediate between lower levels of polarizations where the effect is minimal and hard to notice, and higher polarizations that lead to too high currents. As shown in Figure 12 (a), aged sample shows different exchange activity than that of fresh sample. The amount of $^{18}O_2$ that is detected with the aged sample is lower compared to the amount detected with the fresh sample. At the same time the $^{16}O_2$ level is higher for the aged sample. This indicates that the aged sample is more active through a multiple hetero-exchange:

$$^{18}O_{2(g)} + {}^{16}O_{2(s)} \qquad {}^{16}O_{2(g)} + {}^{18}O_{2(s)} \tag{6}$$

However, at the same time, the level of the scrambled product signal, $^{16}O^{18}O$, is lower for the aged sample. This shows that the activity of the aged sample is slower in the case of a simple hetero-exchange, where only one solid atom participates in the exchange:

$$^{18}O_{2(g)} + {}^{16}O_{(s)} \qquad {}^{16}O^{18}O_{(g)} + {}^{18}O_{(s)} \tag{7}$$

Figure 12 (b) displays the variance in the exchange coefficient of LSCF-GDC along the aging test at 500°C, under polarization of -300mV. As can be seen, there is a continuous decrease in the oxygen exchange

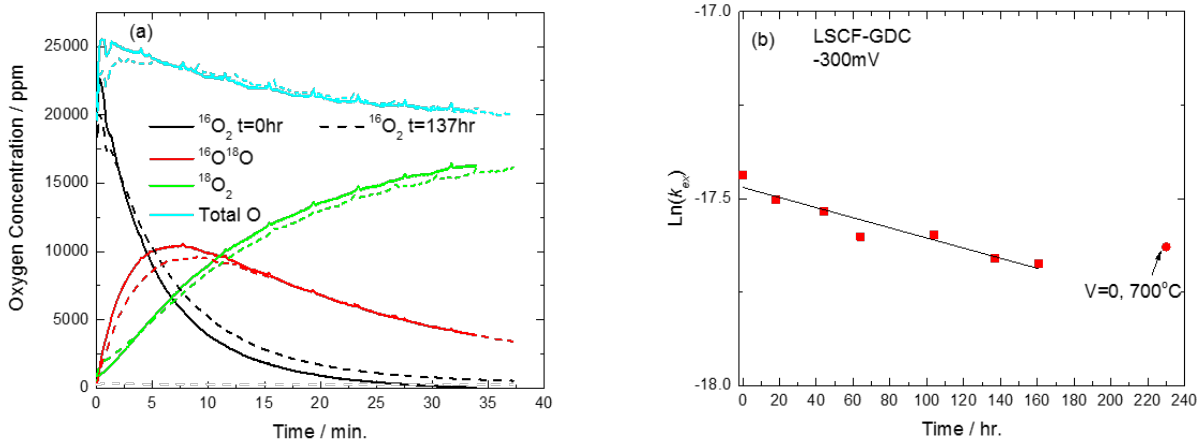

Figure 12. (a) Oxygen isothermal isotope exchange profile for LSCF-GDC at 500°C under cathodic polarization of -300mV before and after aging for 137 hours. (b) Variation of LSCF-GDC oxygen surface exchange coefficient with aging time at 500°C under cathodic polarization of -300mV.

coefficient with time. The total degradation in the value of the exchange coefficient over the entire test time is $5.12*10^{-9}$ (the error in each calculated exchange coefficient value is in the order of 10^{-10} $(cm*sec)^{-1}$. This leads to a calculated degradation of $3.2*10^{-11}$ $(cm*sec)^{-1}$ per hour in the surface exchange. Also included in Figure 12 (b) is the surface exchange coefficient for LSDC-GDC aged at a constant temperature of 700°C for a duration of 230 hours, however without any electrical polarization applied on the sample during aging. The actual measurement of oxygen isotope exchange was conducted under polarization of -300mV. As can be seen, the measured oxygen exchange coefficient after longer aging under open circuit conditions, is higher compared to a sample aged at lower temperature (500°C), shorter time (160 hours) but under cathodic polarization of -300mV. Therefore, for LSCF-GDC, the application of cathodic polarization contributes to higher degradation rates than if those are obtained under open circuit. Under this conditions, the degradation rate in the surface exchange coefficient is only $2.1\cdot10^{-11}$ $(cm*sec)^{-1}$ per hour.

The effect of time and polarization on the oxygen surface exchange of LSCF at 500°C was also examined. Figure 13 (a) exhibits the oxygen exchange profile of LSCF under cathodic polarization of -300mV, before and after aging under this polarization for 140 hours. As can be seen, there is a noticeable difference in the exchange profile. The total concentration of O_2 is higher for the aged sample, which indicates that during the aging process, and especially at the beginning of it, the sample stoichiometry changes and the oxygen level in the sample decreases with time. The curves of the signal species, $^{16}O_2$, $^{16}O^{18}O$, and $^{18}O_2$, show similarity in their general shape, however there is a different evaluation with time for each individual curve. The difference is probably due to changes in the chemical composition of the materials along the aging period, which lead to decrease amount of available oxygen for the exchange reaction in the aged material.

Figure 13 (b), which presents the variation in the oxygen surface exchange coefficient with time, confirms the stated above. As can be seen, along the aging process at 500°C under polarization of -300mV, there is no clear trend in the value of the exchange coefficient. Based on the value of the exchange coefficient after 160 hours at 500°C and -300mV, the calculated degradation rate is $1.05*10^{-10}$ $(cm*sec)^{-1}$

per hour. However the trend changes from decrease in time at the beginning to an increase at longer times. Figure 13 (b) also includes the exchange coefficient of a different sample of LSCF, measured under the same conditions of 500°C under polarization of -300mV, however this sample was aged prior to isotope exchange experiment at 700°C for 230 hours, and no polarization was applied during the aging process. Under this aging mode, there is also a decrease in the exchange rate coefficient, and the degradation rate is

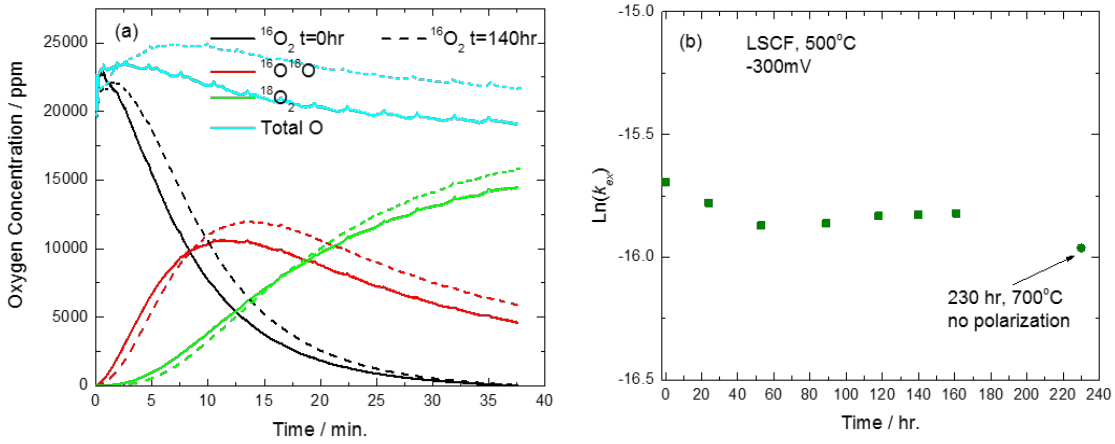

Figure 13. (a) Oxygen isothermal isotope exchange profile for LSCF at 500°C under cathodic polarization of -300mV before and after aging for 140 hours. (b) Variation of LSCF oxygen surface exchange coefficient with aging time at 500°C under cathodic polarization of -300mV, and after 230 hours with no applied polarization.

$1.57 \cdot 10^{-10}$ $(cm*sec)^{-1}$ per hour. These results indicate that for the case of LSCF, the oxygen surface exchange coefficient decreases with time, however this degradation in the exchange activity of the material is not a result of the application of polarization, since the degradation appears also when polarization is not applied.

The effect of time and polarization on the oxygen surface exchange kinetics was examined also for LSM. Since oxygen surface exchange on LSM, unlike on LSCF, is not limited by diffusion of reactants from the gas phase, we were able to test and aged LSM at higher temperature of 700°C. Figure 14 (a) exhibits the oxygen exchange profile of LSM under cathodic polarization of -300mV, before and after aging at this polarization level for 165 hours. As can be seen, for LSM there is a noticeable difference in the exchange profile. The signal represents $^{16}O_2$ decays faster for the aged sample than for the fresh one. The

scrambled product signal, $^{16}O^{18}O$, shows much higher concentration values for the aged sample, compared to the non-aged one. These all are indications of a faster oxygen exchange kinetics for aged LSM.

Figure 14 (b) displays all the calculated surface exchange coefficients for aged LSM, along the aging process at 700°C for 165 hours. As can be seen, even though there is a slight decrease at the beginning of the aging process, the general trend is an increase in the surface exchange coefficient value with aging time. After the 165 hours, the obtained increase rate in the surface exchange is $2*10^{-10}$ $(cm*sec)^{-1}$ per hour. It can also be seen that after 120 hours, the value of the surface exchange coefficient reaches a plateau and stabilizes. We also measured the surface exchange coefficient of LSM aged under no polarization, for longer time of 230 hours at the same temperature. As described in Figure 14 (b), the value of the surface exchange coefficient is similar for the case on aging with no polarization, even though the aging time was longer. Therefore, it cannot be definitely determined whether the increase in the surface exchange coefficient is due to the application of cathodic polarization during the aging process.

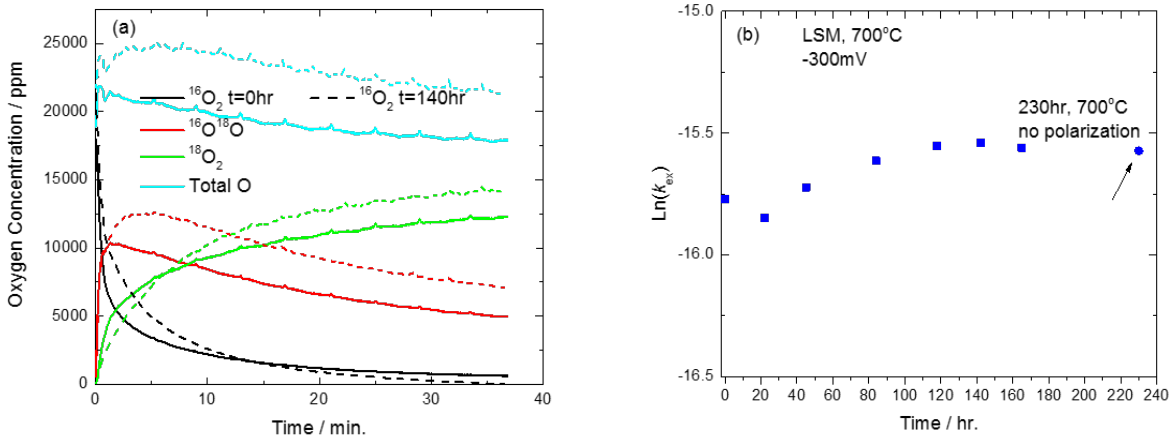

Figure 14. (a) Oxygen isothermal isotope exchange profile for LSM at 700°C under cathodic polarization of -300mV before and after aging for 140 hours. (b) Variation of LSM oxygen surface exchange coefficient with aging time at 700°C under cathodic polarization of -300mV, and after 230 hours with no applied polarization.

5. Conclusions

Application of real time conditions of electrochemical polarizations can cause significant changes to the oxygen surface exchange activity of SOFC cathode materials. We successfully developed a novel *in-operando* measurement system, based on oxygen isotope exchange, with a micro-reactor containing a powder sample of the SOFC cathode material. This micro-reactor also serves as a complete electrochemical cell, providing the ability to apply voltage between the cathode material and a Pt electrode. This configuration enables monitoring and detecting the oxygen surface exchange kinetics of SOFC cathode materials when voltage is applied The analysis of the measured data show that the surface exchange coefficient increases dramatically when cathodic polarization is applied. Following the goals of the project, an appropriate model was developed for the *in-operando* measurement mode, based on movement of oxygen ions due to the electrochemical potential. The acquired data was fitted to this model, using fitting parameters obtained from simple electrochemical measurements. The results reveal that for LSM, LSCF, LSC, and LSF using fitting parameters obtained through simple electrochemical characterization of the materials, the oxygen surface exchange coefficient can be successfully predicted. Moreover, the LSC and LSF results demonstrate that while LSF has a lower surface exchange coefficient at OCP compared to LSC, under applied polarization this is reversed indicating LSF may be a better cathode material. This apparatus also enables the detection of the changes in the oxygen surface exchange properties of cathode materials along long-term aging conditions at high temperatures and under applied polarizations.

Using these apparatus and model, we accomplished our objective to predict the surface oxygen exchange rate coefficient of SOFC cathode materials, as well as their behavior under various working conditions. These predictions can be used to rationally optimize cathode material composition and structure, and subsequently be used to determine and predict cathode degradation mechanisms.

6. References

1. C. Xiong, J.A. Taillon, C. Pellegrinelli, Y. Huang, L.G. Salamanca-Riba, B. Chi, L. Jian, J Pu, and E.D. Wachsman, *J. Electrochem. Soc.* **163**, F1091 (2016).

2. Y. L. Huang, C. Pellegrinelli, and E. D. Wachsman, *J. Electrochem. Soc.* **163**, F171 (2016).

3. Y. L. Huang, C. Pellegrinelli, and E. D. Wachsman, *ACS Catal.* **6**, 6025 (2016).

4. Y. L. Huang, C. Pellegrinelli, and E. D. Wachsman, *Angew.Chem.Int. Ed.* **55**, 15268 (2016).

5. C. Pellegrinelli, Y. L. Huang, J. A. Taillon, L. G. Salamanca-Riba, and E. D. Wachsman, *ECS Trans.* **68**, 773 (2015).

6. E.N. Armstrong, K.L. Duncan and E.D. Wachsman, *Phys.Chem. Chem. Phys*. **15**, 2298 (2013).

7. E.N. Armstrong, K.L. Duncan, D.J. Oh, J.F. Weaver and E.D. Wachsman, *J. Electrochem. Soc.* **158,** B492 (2011).

8. G. Cohn, J. Wang, C. Pellegrinelli, K. Huang, and E.D. Wachsman, *J. Electrochem. Soc.* **163,** F979 (2016).

9. R. Imbihl, *Progress in Surface Science* **85,** 241 (2010).

10. S. Carter, A. Selcuk, R.J. Chater, J. Kajda, J.A. Kilner, and B.C.H. Steele, *Solid State Ionics*, **53–56**, 597 (1992).

11. J.E. ten Elshof, M.H.R. Lankhorst, and H.J.M. Bouwmeester, *J. Electrochem. Soc.*, **144**, 1060 (1997).

12. R.A. De Souza and J.A. Kilner, *Solid State Ionics*, **106**, 175 (1998).

13. A.V. Berenov, A. Atkinson, J.A. Kilner, E. Bucher, and W. Sitte, *Solid State Ionics*, **181**, 819 (2010).